

Unsupervised K -modal Styled Content Generation

Omry Sendik
Tel Aviv University
omrysendik@gmail.com

Dani Lischinski
The Hebrew University of Jerusalem

Daniel Cohen-Or
Tel Aviv University



Figure 1: Samples generated using our unsupervised K -modal GAN (uMM-GAN with $K = 2$) trained on datasets containing two classes: the two letters 'A' & 'B' (left) and Cats & Dogs (right), with each class exhibiting many different styles. Each sample in the bottom row is generated from the same latent vector as the one above it, after swapping between the weights of the learned modes. Using multiple modes to model the data distribution not only improves the quality of the generated samples, but also disentangles mode from style, enabling switching between data modes while preserving various style attributes.

Abstract

The emergence of generative models based on deep neural networks has recently enabled the automatic generation of massive amounts of graphical content, both in 2D and in 3D. Generative Adversarial Networks (GANs) and style control mechanisms, such as Adaptive Instance Normalization (AdaIN), have proved particularly effective in this context, culminating in the state-of-the-art StyleGAN architecture. While such models are able to learn diverse distributions, provided a sufficiently large training set, they are not well-suited for scenarios where the distribution of the training data exhibits a multi-modal behavior. In such cases, reshaping a uniform or normal distribution over the latent space into a complex multi-modal distribution in the data domain is challenging, and the quality of the generated samples may suffer as a result. Furthermore, the different modes are entangled with the other attributes of the data, and thus, mode transitions cannot be well controlled via continuous style parameters. In this paper, we introduce uMM-GAN, a novel architecture designed to better model such multi-modal distributions, in an unsupervised fashion. Building upon the StyleGAN architecture, our network learns multiple modes, in a completely unsupervised manner, and combines them using a set of learned weights. Quite strikingly, we show that this approach is capable of

homing onto the natural modes in the training set, and effectively approximates the complex distribution as a superposition of multiple simple ones. We demonstrate that uMM-GAN copes better with multi-modal distributions, while at the same time disentangling between the modes and their style, thereby providing an independent degree of control over the generated content.

1. Introduction

Content generation has been a major bottleneck since the dawn of computer graphics. Recently, the emergence of generative models based on deep neural networks, finally carries a promise for being able to automatically generate massive amounts of diverse content. Although the visual quality of deep generative models could not initially rise up to the high visual fidelity bar of the field, it has been improving rapidly. Some of the most promising approaches, in terms of visual fidelity are Generative Adversarial Networks (GANs) [4], which learn to generate samples whose distribution closely resembles that of the training data.

While GANs are able to generate a large amount of varied data, provided a sufficiently large training set, they are not explicitly designed for scenarios where the distribution of training data exhibits a multi-modal behavior. Consider, for example, a dataset consisting of several different species

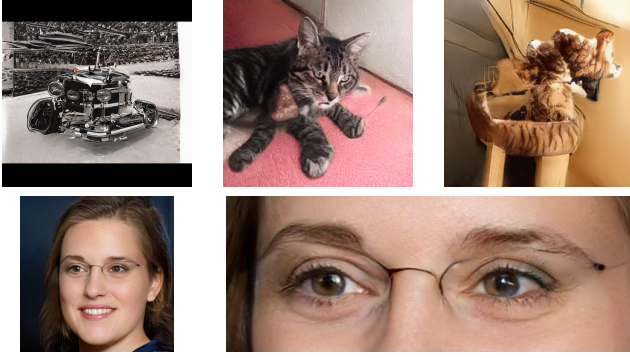


Figure 2: StyleGAN failure cases: The top row shows a car on the left, and two cats on the right, all of which were generated by trained models provided by Karras *et al.* [9]. In the bottom row, we attribute the partial presence of eye-glasses to the dataset having two distinct modes.

of animals, or several different kinds of cars. In such cases, reshaping a simple distribution over the latent space into a complex multi-modal one is challenging, reducing the quality of the synthesized result. A number of works note and attempt to address this issue, as briefly reviewed in Section 2.

Furthermore, the control that GANs typically provide over the generated data is limited, especially in the unsupervised learning scenario, i.e., when the data comes without any additional annotations. A degree of control may be achieved by adding conditioning [15]. However, this requires supervision, which is not always feasible.

Karras *et al.* [9] recently introduced StyleGAN, an unsupervised framework that leverages the AdaIN style control mechanism [7] to afford some degree of control over attributes at different scales. By first mapping a simply distributed latent space into an intermediate one, they are able to better approximate the training probability density, while avoiding entangling the factors of variation. The StyleGAN architecture has resulted in the highest quality data-driven generative models to date. However, warping a simple distribution into a non-convex multi-modal one may result in synthesis failures, as demonstrated in Figure 2. For example, in a dataset of cat images, the diversity of cat poses is a possible reason for the generation failures shown in the top row. Similarly, the presence or absence of glasses in a face dataset defines two distinct modes in the training distribution, which may result in faces with partial glasses.

In this work, we introduce a new generative model, designed explicitly for coping with multi-modal distributions. For such distributions, our model results in higher quality synthesis, in addition to providing the ability to directly control the mode of the generated samples, independently of the control afforded by the style parameters. Remark-

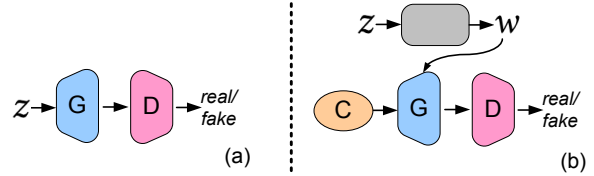


Figure 3: (a) The original GAN architecture proposed by Goodfellow *et al.* [4]. (b) The StyleGAN of Karras *et al.* [9], which is composed of a mapping network (from $z \in \mathcal{Z}$ to $w \in \mathcal{W}$) and a synthesis network, fed by a learned root constant C . The synthesis is controlled using AdaIN parameters derived from w .

ably, our approach requires no supervision; provided only the number of modes K as a hyper-parameter, it is able to learn the different latent modes in the training distribution, while learning to generate samples resulting from them.

Specifically, the architecture that we introduce here is based on that of StyleGAN [9]. The StyleGAN generator uses a single learned constant that serves as a common seed or *root* for all of the synthesized samples from a given distribution. All the variations among the generated samples result from varying AdaIN parameters, as well as random noise inputs, at each generation scale. In contrast, we propose to learn K *root constants*, which may be interpreted as seeds for the different modes present in the data. Intuitively, rather than relying on the ability of the mapping network to deform the latent space distribution into one that follows the training probability density, we approximate the latter using a composition of simpler distributions around multiple modes.

We show that our K -rooted generators are able to produce higher quality samples for multi-modal distributions, compared with the state-of-the-art. Perhaps more importantly, we show that the root constants in our architecture correspond to different modes in the training set. Finally, spanning the learned distribution in this manner, results in an explicit method for controlling the mode of the generated data, providing a new degree of control which is natural for multi-modal distributions, and has little or no effect on the attributes controlled via AdaIN and noise, as demonstrated in Figure . Thus, our approach effectively disentangles mode and “style”.

2. Background

We explore the problem of unsupervised generation of natural images. Research in this area received a tremendous boost with the introduction of Generative Adversarial Networks (GANs) [4]. Given a set of training samples, GANs learn to generate samples whose distribution closely resembles that of the training data. The commonly used DCGAN

architecture [19], summarized in Figure 3(a), consists of a convolutional generator G , fed by a random input vector $z \in \mathcal{Z}$, typically drawn from a normal or a uniform distribution. The generator is adversarially trained using a convolutional discriminator D .

Such GAN architectures are able to learn to sample sufficiently restricted distributions, however, they are not well suited for distributions that exhibit significant diversity or multi-modal behavior. Multi-modal distributions may be sampled using conditional GANs [15], provided that the training data is suitably annotated, for example with class labels. For example, Odena *et al.* [17] concatenate a one-hot class vector to the generator’s noise input. Brock *et al.* [2] have demonstrated that class-conditioning makes it possible to effectively sample distributions as diverse as ImageNet [20].

This limitation of GANs has been discussed by multiple researchers (e.g., [5, 1, 10, 18]). Several works, such as [1, 5, 18], cope with the multi-modal case by structuring the latent space \mathcal{Z} as a Mixture of Gaussians, whose first and second moments are learned. While some of these approaches are unsupervised, they impose a specific parametric model on the latent distribution, and mostly assume that the data consists of disconnected clusters or manifolds. Contrary to these works, our approach makes no a priori assumptions regarding the form of the distribution (i.e., we do not assume it is a Gaussian Mixture Model). Neither do we assume that the distribution consists of several disconnected parts. In addition, our approach is unique in that it enables disentangled control of mode and other visual attributes.

Brock *et al.* [2] note that the choice of latent space might significantly affect the performance of GANs. In particular, they observed that the discrete Bernoulli $\{0, 1\}$ latent space outperformed the normal distribution (without truncation), arguing that it might reflect the prior that the underlying factors of variation in natural images are discrete (one feature is present, another is not). In our approach there is no need to choose between continuous and discrete distributions, since both the modes and their mixture are learned by the network. Thus, the network adapts itself to the training data, rather than being pre-designed for a particular kind of distribution.

In addition to GANs, a variety of alternative generative models have also been explored. Notable examples include Variational Auto-Encoders (VAEs) [12], and variants thereof that attempt to achieve clustering in the latent space, such as GMVAE [3], or ClusterGAN [16], which combines the advantages of VAEs and GANs. Another unique work in the line of Generative models is Glow [11]. By using 1×1 invertible convolutions within a flow-based generative model, Kingma *et al.* have demonstrated that a generative model is capable of efficiently synthesizing realistic-looking images. None of the above methods, however, were able to demon-



Figure 4: Images generated by different StyleGAN models using an average style vector w_{avg} (obtained by drawing a large number of z vectors and averaging their corresponding w vectors).

strate the high-resolution sharp images, such as those that may be produced by the latest GANs.

2.1. StyleGAN

The state-of-the-art in GAN-based image generation is achieved by the StyleGAN architecture [9], a fascinating combination between GANs and the AdaIN mechanism [7]. The StyleGAN architecture, diagrammed in Figure 3(b), first maps the latent vectors z , normally or uniformly distributed in a latent space \mathcal{Z} , into an properly shaped intermediate latent representation $w \in \mathcal{W}$, using a learned mapping network. The w vectors are then transformed into sets of AdaIN parameters, originally introduced in the context of style transfer, which are injected into the different levels of the generator.

Notably, the generator takes as input a single (learned) constant, which we refer to as the *root constant*. The root constant may be seen as an encoding of the learned mode of the training data. Figure 4 visualizes this learned mode for several StyleGAN models trained by Karras *et al.* on different datasets (faces, bedrooms, cars, and cats). The visualization is obtained by feeding the generator network G with an average style vector w_{avg} , and without noise inputs. For example, note that the generated face shown in Figure 4 is neither very masculine nor very feminine and its complexion is not very dark or very pale. Under normal operation, the generator is able to shift away from these average properties through the use of different sets of AdaIN parameters, obtained by transforming different vectors $w \in \mathcal{W}$. Thus, to model a given distribution well, the shape of the distribution should be echoed by that of the intermediate latent space \mathcal{W} .

StyleGAN has been shown to perform admirably on several image domains, however, we note that it is still best suited for distributions with a single dominant mode, as we shall demonstrate in the next section. In contrast, in this work we are interested in multi-modal domains, where the modes might correspond to distinct peaks in the probability density, or might span the probability density in a more continuous manner. In either case, the training data samples typically share some common attributes, which span across modes. Consider a set of fonts, for example. Within each font, letters share common properties, such as font-weight,

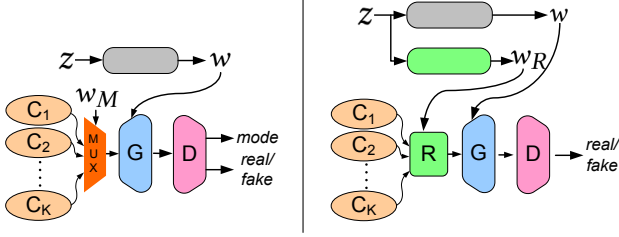


Figure 5: Our Multi-Modal GAN architecture borrows from StyleGAN the generator G , discriminator D and the mapping network that maps $z \in \mathcal{Z}$ to $w \in \mathcal{W}$. In place of a single constant input to G , K root constants are learned. **Left:** In the supervised variant, one of the K constants is selected by a multiplexer and forwarded to G . Note that the discriminator penalizes the generator at train time on its generated modes. **Right:** In the unsupervised variant, the K learned constants are blended by R , using a vector of weights w_R to yield the input of G . The blending weights w_R are generated by a mapping network, with a softmax as its last layer.

style and character dimensions. However, the distribution is multi-modal, where each character defines a separate mode. In cases such as this, the distribution is unlikely to be well approximated by a set of multiscale variations around a single mode. Consequently, attempting to train a single model on the entirety of such a dataset (without supervision such as class-conditioning) might lead to implausible results, as demonstrated in Figures 2 and 9(a).

3. Mode Mixture Modeling

We argue that the single constant learned by StyleGAN is actually an encoding of the representative content of the training data, or, in other words, the single mode of the distribution. The mode may be visualized by letting each trained model generate a sample using a set of average style parameters, as shown in Figure 4.

Instead, we aim to represent the learned distribution using a model which is an explicit mixture of modes. Rather than expecting the mapping network to learn a complex deformation of the latent space, our architecture explicitly reflects the fact that the distribution is modeled using K modes, by training a generator that takes K learned root constants as input, instead of a single one. The K constants are mixed using a set of learned weights and the resulting mixtures are further modified by a common set of style (AdaIN) parameters to generate samples that cover the entire learned distribution. If the distribution is roughly discrete, and the training data is annotated accordingly, the corresponding constants and their mixture may be learned in a supervised fashion. However, as we show in Section 3.1, supervision is actually not necessary.

3.1. Multi-Modal GAN

We begin by describing a supervised version of our Multi-Modal GAN (sMM-GAN), which may be suitable for the case where the data modes correspond to distinct clusters, and each training sample is annotated with the mode to which it belongs. This supervised architecture is depicted in the left diagram in Figure 5. The architecture borrows from StyleGAN its generator G and the mapping network that maps \mathcal{Z} to \mathcal{W} . However, in place of a single constant input to G , K root constants, denoted C_1, \dots, C_K are learned, which are intended to encode up to K modes of the distribution. A one-hot vector w_M controls a simple multiplexer that chooses one of these K constants to be forwarded as input to G . In order to learn K constants that would correspond to K modes in the data, we add a K -way classifier to the discriminator D , which is used to penalize the generator when it fails to produce an image that does not belong to the mode indicated by w_M .

Our main goal, however, is to learn the mode mixture model in an unsupervised fashion. This is accomplished by the unsupervised version of Multi-Modal GAN (uMM-GAN), depicted in the right diagram of Figure 5. As before, we learn K root constants; however, in this variant, these constants are fed into a blending layer (denoted R), where they are blended using K weights w_R , and the resulting blended vector is fed into the generator G . The weights w_R are generated from the latent vectors $z \in \mathcal{Z}$ using a mapping network parallel to the one that maps \mathcal{Z} to \mathcal{W} , and ended by a softmax layer that normalizes the selection weights to a sum of one.

The advantage of our uMM-GAN over the original StyleGAN is demonstrated in Figure 6 using a simple synthetic example. The training samples have a simple parameterization in 2D and are drawn from a continuous probability density function (PDF), which nevertheless exhibits a complex anisotropic shape in the plane.

Specifically, each sample is an image with two white rectangles of the same height, but varying widths (such as the images shown in the bottom row of Figure 6). Thus, the widths of the two rectangles provide a natural embedding of the training set on the plane. The width of one rectangle (Width 1) is uniformly sampled from $[0, 40]$, while the range of widths of the second rectangle (Width 2) depends on Width 1. The joint PDF of the two widths forms the shape of the letter H, as shown in the top left image of Figure 6.

Having drawn 10,000 samples from this distribution, the resulting set of images is used to train a StyleGAN, as well as a uMM-GAN (with $K = 3$). Visualizing the empirical PDFs sampled by these two generative models, we can see that StyleGAN is unable to faithfully reproduce the training distribution (top row, middle). In contrast, the PDF of uMM-GAN with $K = 3$ approximates the training PDF

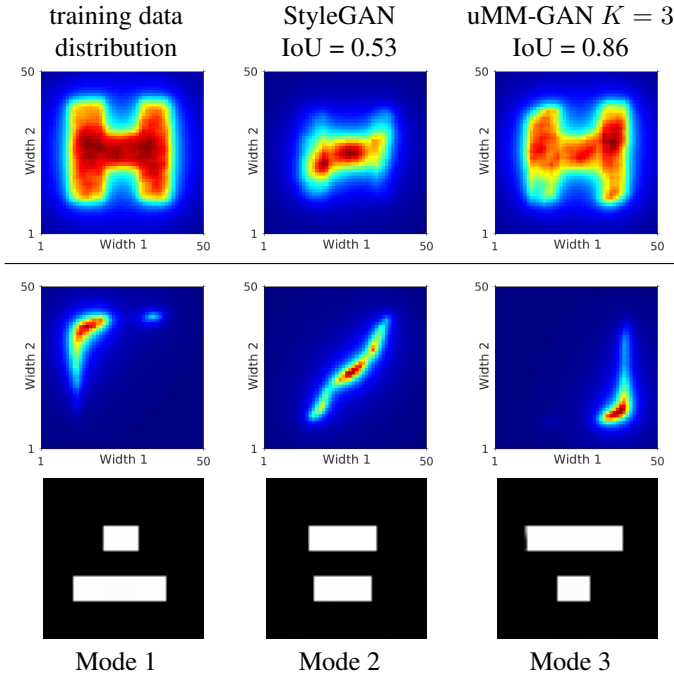


Figure 6: Effect of multi-modal generation. We form a dataset with a 2D parameterization, and an H-shaped distribution (top left). Training StyleGAN on this dataset reproduces only a part of the distribution (top middle), while training uMM-GAN with $K = 3$ results in a much better approximation, and a higher Jaccard index value (IoU). The three learned modes are visualized in the middle and bottom rows. The middle row visualizes the distributions that are sampled by replacing the blending weights vector w_R with a one-hot vector. The mixture of the resulting distributions is able to reproduce the H-shape. The bottom row shows the generated samples corresponding to the three learned constants.

quite well (top row, right). In order to quantify the fit, we apply a threshold over the PDFs and compute the Jaccard index (Intersection over Union) between the training PDF and that of the two generated ones, resulting in an index of 0.86 for uMM-GAN, compared to 0.53 for StyleGAN.

It is also instructive to examine the PDFs generated by uMM-GAN around each of the three modes that it has learned, visualized in the middle row of Figure 6. Note that the shape of each PDF covers a different part of the H shape, facilitating the approximation of the anisotropic training PDF as a superposition of three simpler ones. Also note, that the shapes of the three PDFs are learned by the network, and they differ from a 2D Gaussian, as well as from each other. The images corresponding to each of the three modes are shown in the bottom row of Figure 6.

3.2. Disentanglement of mode and “style”

The mode and the style in a heterogeneous dataset are often naturally disentangled. For example, consider a dataset consisting of cats and dogs (two different content modes), where some of the cats and the dogs may have similar looking fur patterns, colors, etc. In the StyleGAN architecture, some degree of disentanglement between different factors of variation is achieved by the mapping network that deforms the simply distributed latent space \mathcal{Z} into the intermediate latent space \mathcal{W} , which may have a more complicated shape (refer to Figure 6 or [9]). However, the use of a single root constant makes it difficult to disentangle between variations in style and variations in the mode, which often correspond to content variations. By replacing the single root constant of StyleGAN by a combination of multiple learned root constants, we effectively enable the network to better emulate such disentanglement.

This ability is demonstrated in Figure 7. The top row of nine images was generated using the same mode mixture vector w_R (mapped from a random latent vector $z \in \mathcal{Z}$), while the bottom row was generated using the vector $1 - w_R$. Each of the nine columns corresponds to a different style vector w . Indeed, it is easily observed that in each row the mode (cat or dog) is preserved, while the style (fur colors and patterns) changes. In contrast, along each column, the fur colors and patterns remains similar, while the mode is flipped. It should be noted that while, for this dataset, the two learned modes correspond to the two semantic image classes, this is not guaranteed to be the case in general. In other words, the modes learned by the generator might reflect a different clustering of the data than the one that might be more readily perceived by a human observer.

4. Results

We implemented the Multi-Modal GAN architectures discussed in the previous sections in PyTorch. It should be noted that the original StyleGAN of Karras *et al.* [9] is a special case of our uMM-GAN architecture, with $K = 1$. For the StyleGAN and Multi-Modal GAN models, all of the results reported below were obtained by training for 200,000 iterations, in a progressively growing manner [8]. Glow models were trained for 200,000 iterations but without progressive growing. All of the models we compare to were trained using the hyper-parameters which were proposed by the original authors.

For comparing between different generative models, we make use of the widely accepted FID metric [6]. Each FID score is calculated on two sets (real and fake) of 5000 images. Throughout this section, we refer to the (empirical) number of modes in our multi-modal datasets as N (not to be confused with K , which denotes the number of constants



Figure 7: Disentanglement of mode and style: The top row of nine images was generated using the same mode mixture vector w_R (mapped from a random latent vector $z \in \mathcal{Z}$), while the bottom row was generated using the vector $1 - w_R$. Each of the nine columns corresponds to a different style vector w (mapped from nine random vectors in \mathcal{Z}). In each row, the mode (cat or dog) remains the same, while the style changes. In each column, the fur colors and patterns are similar, while the mode is flipped.

		StyleGAN	Two StyleGANs	Glow	sMM-GAN	uMM-GAN
Letters	FID	36.15	36.03	45.63	32.09	33.13
	Samples					
Dogs & Cats	FID	126.90	120.44	123.75	107.94	117.25
	Samples					

Figure 8: Performance of different generative models on two bi-modal datasets. From left to right, the architectures are: StyleGAN, two StyleGANs (each trained on part of the dataset containing a single mode), Glow, our supervised sMM-GAN, and our unsupervised uMM-GAN. The dataset in the top row consists of two letters ‘A’ and ‘B’, handwritten in a variety of styles. The dataset in the bottom row consists of portraits of dogs and cats (from DRIT [13]).

in our models). For all experiments on images of handwritten characters, the output of all generators and the input of all discriminators was changed to grayscale images of 64×64 pixels. Our remaining images/generators all use the resolution of 128×128 , unless stated otherwise. This resolution was chosen due to limited computational resources available to us, but it is not an inherent limitation.

We found the truncation trick, which was used by Brock *et al.* [2] and Karras *et al.* [9], helpful for improving quality. Thus, all of the images shown hereinafter, both from our models and from models we compare to, are produced

using truncation.

4.1. Generation Quality

We begin by comparing the quality of the results generated by StyleGAN [9] and Glow [11] to those generated by sMM-GAN and uMM-GAN, when trained on bi-modal datasets containing images from two classes: our own dataset of handwritten letters ‘A’ and ‘B’, and the Cats & Dogs dataset from DRIT [14]. Since each of these datasets consists of two distinct classes, we also compare with two StyleGAN models, each trained only on half of

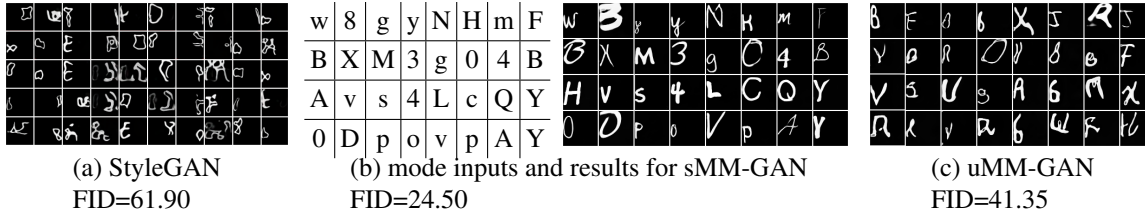


Figure 9: Results of StyleGAN, sMM-GAN, and uMM-GAN, on a dataset of 62 characters. (a) Samples generated by StyleGAN are clearly implausible. (b) the conditional mode inputs w_M to sMM-GAN and the corresponding results. Adding multiple roots and supervision in sMM-GAN vastly improves the results. Note that w_M properly controls the desired output. (c) The results of uMM-GAN are clearly better than StyleGAN, but seem to be slightly degraded compared to sMM-GAN, due to the removal of the supervision. We also report the FID scores of each model, showing the benefit of multiple roots.

each dataset that consists of images from the same single class. The results of this experiment are summarized in Figure 8.

It may be seen that some of the images generated by a single StyleGAN do not look like plausible handwritten letters ‘A’ or ‘B’. This is also true for some of the Cats/Dogs results, where some of the generated images look like a mixture between a dog and a cat (see for example the bottom image in the second column from the left). Quantitatively, the single StyleGAN results in the highest (worst) FID score (among the GAN-based methods), for both datasets.

When training two StyleGAN models on each dataset (split accordingly), the visual results are improved only slightly, and the reduction in the FID score is also quite small. We hypothesize that the reason for this is that the two separate models have more degrees of freedom, and fail to leverage the style commonalities present across the entire multi-modal input distribution. An additional factor might be that each of the two StyleGAN models in this case was trained on only half the number of training samples.

The visual results generated by Glow, appear to be blurrier than the training samples. Quantitatively, the FID scores are the worst for the A/B dataset, and second worst for the Cats/Dogs. It should also be noted that some of the images generated by Glow were completely black; we filtered these results out, before computing the FID scores.

Compared to these tested alternatives, both our multi-modal architectures (sMM-GAN and uMM-GAN) exhibit better performance. The generated handwritten letters appear much more clear and plausible, while our Cats/Dogs results are more consistent in the sense that our models’ resulting output breed is more easily determinable. The FID scores for both our architectures are lower (better) as well. Naturally, the supervised variant, sMM-GAN, results in better FID scores than the unsupervised uMM-GAN. We attribute the improved performance of uMM-GAN compared to the unimodal StyleGANs to the fact that it is able to benefit from learning the joint visual attributes of both classes in each dataset, without being constrained to synthesize both

classes from a single learned constant.

We have also experimented with a dataset consisting of a large number of distinct classes. Figure 9 compares the results of StyleGAN to those generated by sMM-GAN and uMM-GAN, where all three architectures are trained on a dataset of 62 characters. The dataset consists of 216 different fonts, with a total of 14,000 letters. This dataset was manually curated by ourselves and will be made public upon publication of this work.

Figure 9(a) clearly demonstrates that the results of StyleGAN trained on a dataset with that many different modes are implausible, as almost none of the generated images resemble a character from the dataset. Figure 9(b) show the desired mode as indicated by the mode vector w_M and the corresponding results generated by sMM-GAN. The results are significantly better, and it is apparent that the desired mode is generated. Figure 9(c) shows the results generated by uMM-GAN. While the results are slightly degraded compared to (b), they are still clearly more plausible than those of the unimodal StyleGAN. Additionally, we report the FID score obtained by each of the three models, showing that uMM-GAN improves upon StyleGAN and that, thanks to supervision, sMM-GAN outperforms both.

4.2. Learnt Modes

At the basis of our approach is the assumption that the learned constants encode a template or a canonical representation of the modes present in the dataset from which we wish to sample and generate images. In order to visually demonstrate this, we visualize the constants learned by StyleGAN and by uMM-GAN for two bi-modal datasets. This is done by computing and applying an *average style vector* $w_{\text{avg}} \in \mathcal{W}$, obtained by running 10,000 random latent vectors $z \in \mathcal{Z}$ through the mapping network of each generator and averaging the results. Next, we disable the noise inputs to the synthesis network of the generator and apply the AdaIN parameters resulting from w_{avg} . Thus, the generator “renders” its learnt constant using an “average” style. When we apply this method on our uMM-GAN, we

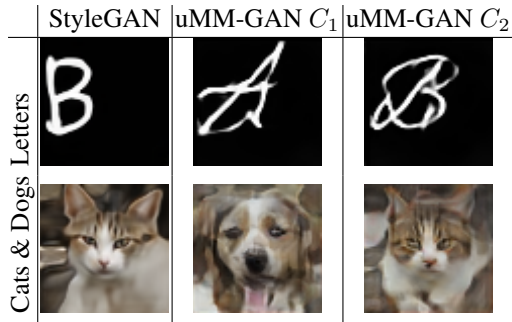


Figure 10: Visualization of constants learned by StyleGAN and uMM-GAN for two bi-modal datasets. We first compute an *average style vector* $w_{\text{avg}} \in \mathcal{W}$, by running 10,000 random latent vectors $z \in \mathcal{Z}$ through the mapping network of each generator and averaging the results. Next, we disable the noise inputs to the synthesis network of the generator and apply the AdaIN parameters resulting from w_{avg} . For uMM-GAN, a one-hot vector is used in place of the mixing vector w_R to select one of the two constants to be fed into the generator.

force the generator to select one out of the K learned constants by setting w_R to a corresponding one-hot vector (note that the generation of the style vectors w does not require the value of the mixing vectors w_R).

In Figure 10, we show the resulting average style images for StyleGAN and for our uMM-GAN. It is apparent that StyleGAN (left column), has preferred to learn a constant which perfectly represents one out of the two modes in our datasets. When trained on a dataset with two letters, StyleGAN has learned the average image of one of the two letters ('B'), and when trained on a dataset of cats and dogs, it has learned an average representation of a cat. This implies that in order to generate an image of the letter 'A' or of a dog, StyleGAN must exert substantial effort in order to warp and texture the output properly, using only multi-scale AdaIN parameters. uMM-GAN, on the other hand, has learned two very different modes, which better reflect the modes in our dataset. In the case of a dataset with the letters 'A' and 'B', the two learnt average images resemble the shapes of these two letters. Similarly, when trained on the cats and dogs dataset, an average cat and an average dog are learned. This effectively simplifies our generator's task of properly generating either one of the two classes. We attribute the improvement achieved by our method to this simplification. Recall that learning the two root constants is achieved in an unsupervised manner. In other words, our uMM-GAN is able to uncover two modes with which it spans the distribution of the dataset without any guidance.

4.3. Number of Modes

In Table 1, we report the FID scores obtained by training our uMM-GAN with varying numbers of root constants ($K \in \{2, 3, 4\}$), i.e., learned modes, on datasets with varying numbers of classes ($N \in \{2, 3, 4\}$). Each of these datasets consists of images of N different letters. It is each composed of 216 images of each letter type.

By examining the FID scores in each row of Table 1, it is apparent that for a fixed number of classes (modes) in the dataset, increasing the number of learned modes K improves the results. This behavior is similar to that of clustering algorithms, where increasing the number of clusters typically results in a better fit of the data. It is interesting to note that the largest improvements occur when we move from a model where $K < N$ to one where $N \leq K$. For example, for the case $N = 3$ a drop of 1.47 in the FID score is observed when switching from $K = 2$ to $K = 3$, while increasing to $K = 4$ results in only a modest further reduction (0.4). The same behavior may be observed in the last row ($N = 4$).

By examining the columns of Table 1 one may notice that increasing the number of classes in the dataset, while keeping the same number of learned modes K , results in reduced performance. We believe that this is caused by the increase in the generator's difficulty to cope with the added complexity and richness of the dataset. We stress that in this experiment, a dataset with a smaller value of N , is a subset of those with a larger N . For example, when increasing N from two to three, we simply add another letter to the two already existing ones. This property is important, since it allows us to add new classes, without altering any property of the existing ones.

In Table 2, we report the FID scores obtained by training our uMM-GAN with varying numbers of root constants ($K \in \{2, 4, 8\}$) on the DRIT Cats & Dogs dataset. It is easily noticeable that, similarly to clustering methods, increasing the number of roots improves the FID score, due to the ability to more closely fit the data distribution observed in the training set. Note that the FID scores for the Cats & Dogs dataset are larger than those in Table 1, due to the increased visual complexity of the images.

$K = 1$	$K = 2$	$K = 4$	$K = 8$	$K = 16$
126.90	117.25	109.42	106.44	106.21

Table 2: The effect of increasing the number of constants K learned by uMM-GAN, on the DRIT Cats & Dogs dataset. For each value of K we report the FID score. It is apparent that increasing K improves the score, similarly to unsupervised clustering methods.

	$K = 2$	$K = 3$	$K = 4$
$N = 2$	33.13	32.56	31.62
$N = 3$	34.41	32.94	32.54
$N = 4$	36.78	36.66	34.98

Table 1: The effect of selecting the number of constants K learned by uMM-GAN, as a function of the number of classes N in the training set. For each combination of N and K we report the FID score. By examining the scores in each row, it is apparent that for a fixed number of classes in the dataset, increasing K improves the score. Note also that the largest improvement in the FID score is achieved when we move from $K < N$ to $N \leq K$ (the gray cells on the diagonal). Additionally, by examining columns we may notice that increasing the number of classes in the dataset for a fixed value of K hurts the performance.

4.4. Disentanglement of Mode and Style

As already discussed in Section 3.1, the use of multiple learned root constants in our uMM-GAN not only results in a better approximation of the training distribution, but also provides another degree of control, over the mode of the generated samples, independent of their other visual attributes that are spanned by the style parameters. This is demonstrated in Figures 6 and 7.

Each column (pair) of images in Figure 6 was generated by uMM-GAN with $K = 2$ trained on two bi-modal datasets (the letters ‘A’ & ‘B’, and Cats & Dogs from DRIT [13]). To generate each pair, the same z is randomly drawn and mapped to produce a style vector w and a mixture vector w_R . Next, two images are generated by feeding w_R and $(1 - w_R)$ to the generator. In both bi-modal datasets shown in Figure 6, switching from w_R to $(1 - w_R)$ results in switching the class of the generated image. However, it is apparent that the other visual attributes of the generated image remain largely unchanged. These attributes include the thickness of the stroke in the letters, and the fur and background colors of the pets. It should be noted that the results have been manually arranged such that images of the letter ‘A’ and of cats appear in the top row. This was only done for the sake of the readers’ convenience, and we do not claim to have explicit control over the output class, but rather only the ability to switch the mode.

Another experiment demonstrating the ability of our generator to disentangle mode and style is shown in Figure 7, and was already discussed in Section 3.1.

5. Conclusions

We have presented a novel architecture which targets multi-modal distributions. Our approach makes no a pri-

ori assumptions regarding the form of the distribution, or whether or not the probability density function is continuous or consists of disjoint peaks. Our method has been shown to learn modes which may be used to span the target distribution observed in the training dataset in an unsupervised fashion, requiring only the number of modes to be specified.

Our multi-modal architecture grants the ability to change the modes, which may or may not correspond to semantic content, independently of the style/attributes of the generated output, even when these attributes are shared across different modes.

We have shown that explicit treatment of multiple modes aids the generation process and increases the quality of the produced images. However, the number of modes K must be determined beforehand. It seems summoned to attempt to extend our method to learn the best value of K . Furthermore, more interesting questions arise, like for example, what is the trade off of increasing K . Clearly, an overly large K has a diminishing return, and can lead to an overfit. In the future, we plan to explore the design space of K , and the development of means to set K automatically.

References

- [1] M. Ben-Yosef and D. Weinshall. Gaussian mixture generative adversarial networks for diverse datasets, and the unsupervised clustering of images. *arXiv preprint arXiv:1808.10356*, 2018.
- [2] A. Brock, J. Donahue, and K. Simonyan. Large scale GAN training for high fidelity natural image synthesis. *ICLR*, 2019.
- [3] N. Dilokthanakul, P. A. M. Mediano, M. Garnelo, M. C. H. Lee, H. Salimbeni, K. Arulkumaran, and M. Shanahan. Deep unsupervised clustering with gaussian mixture variational autoencoders. *CoRR*, abs/1611.02648, 2016.
- [4] I. Goodfellow, J. Pouget-Abadie, M. Mirza, B. Xu, D. Warde-Farley, S. Ozair, A. Courville, and Y. Bengio. Generative adversarial nets. In *Advances in Neural Information Processing Systems*, pages 2672–2680, 2014.
- [5] S. Gurumurthy, R. Kiran Sarvadevabhatla, and R. Venkatesh Babu. DeLiGAN: generative adversarial networks for diverse and limited data. In *Proceedings of the IEEE Conference on Computer Vision and Pattern Recognition*, pages 166–174, 2017.
- [6] M. Heusel, H. Ramsauer, T. Unterthiner, B. Nessler, and S. Hochreiter. GANs trained by a two time-scale update rule converge to a local Nash equilibrium. In *Advances in Neural Information Processing Systems*, pages 6626–6637, 2017.

- [7] X. Huang and S. Belongie. Arbitrary style transfer in real-time with adaptive instance normalization. In *Proc. ICCV*, pages 1501–1510, 2017.
- [8] T. Karras, T. Aila, S. Laine, and J. Lehtinen. Progressive growing of GANs for improved quality, stability, and variation. *arXiv preprint arXiv:1710.10196*, 2017.
- [9] T. Karras, S. Laine, and T. Aila. A style-based generator architecture for generative adversarial networks. In *Proc. CVPR*, pages 4401–4410, 2019.
- [10] M. Khayatkhoei, M. K. Singh, and A. Elgammal. Disconnected manifold learning for generative adversarial networks. In S. Bengio, H. Wallach, H. Larochelle, K. Grauman, N. Cesa-Bianchi, and R. Garnett, editors, *Advances in Neural Information Processing Systems 31*, pages 7354–7364. Curran Associates, Inc., 2018.
- [11] D. P. Kingma and P. Dhariwal. Glow: Generative flow with invertible 1x1 convolutions. In *Advances in Neural Information Processing Systems*, pages 10215–10224, 2018.
- [12] D. P. Kingma and M. Welling. Auto-encoding variational bayes. In *2nd International Conference on Learning Representations, ICLR 2014, Banff, AB, Canada, April 14-16, 2014, Conference Track Proceedings*, 2014.
- [13] H.-Y. Lee, H.-Y. Tseng, J.-B. Huang, M. Singh, and M.-H. Yang. Diverse image-to-image translation via disentangled representations. In *Proc. ECCV*, pages 35–51, 2018.
- [14] H.-Y. Lee, H.-Y. Tseng, Q. Mao, J.-B. Huang, Y.-D. Lu, M. K. Singh, and M.-H. Yang. DRIT++: diverse image-to-image translation via disentangled representations. *arXiv preprint arXiv:1905.01270*, 2019.
- [15] M. Mirza and S. Osindero. Conditional generative adversarial nets. *arXiv preprint arXiv:1411.1784*, 2014.
- [16] S. Mukherjee, H. Asnani, E. Lin, and S. Kannan. ClusterGAN: latent space clustering in generative adversarial networks. *CoRR*, abs/1809.03627, 2018.
- [17] A. Odena, C. Olah, and J. Shlens. Conditional image synthesis with auxiliary classifier gans. 2016.
- [18] T. Pandeva and M. Schubert. MMGAN: generative adversarial networks for multi-modal distributions. 2019.
- [19] A. Radford, L. Metz, and S. Chintala. Unsupervised Representation Learning with Deep Convolutional Generative Adversarial Networks. *arXiv.org*, Nov. 2015.
- [20] O. Russakovsky, J. Deng, H. Su, J. Krause, S. Satheesh, S. Ma, Z. Huang, A. Karpathy, A. Khosla, M. Bernstein, A. C. Berg, and L. Fei-Fei. ImageNet Large Scale Visual Recognition Challenge.

International Journal of Computer Vision (IJCV), 115(3):211–252, 2015.